

# Time evolution of the extremely diluted Blume-Emery-Griffiths neural network

D. Bollé<sup>1</sup>, D. R. C. Dominguez<sup>2</sup>, R. Erichsen Jr.<sup>3</sup>  
E. Korutcheva<sup>4</sup> \* and W. K. Theumann<sup>3</sup>

<sup>1</sup>*Instituut voor Theoretische Fysica, Katholieke Universiteit Leuven, B-3001 Leuven, Belgium*

<sup>2</sup>*E.T.S. Informática, Universidad Autónoma de Madrid, Cantoblanco, 28049 Madrid, Spain*

<sup>3</sup>*Instituto de Física, Universidade Federal do Rio Grande do Sul, Caixa Postal 15051. 91501-970 Porto Alegre, RS, Brazil*

<sup>4</sup>*Departamento de Física Fundamental, UNED, c/Senda del Rey No. 9, 28080, Madrid, Spain*

(March 22, 2022)

The time evolution of the extremely diluted Blume-Emery-Griffiths neural network model is studied, and a detailed equilibrium phase diagram is obtained exhibiting pattern retrieval, fluctuation retrieval and self-sustained activity phases. It is shown that saddle-point solutions associated with fluctuation overlaps slow down considerably the flow of the network states towards the retrieval fixed points. A comparison of the performance with other three-state networks is also presented.

## I. INTRODUCTION

There has been much interest in understanding the properties and predicting the behavior of large attractor neural networks. Of primary concern are the storage capacity, the ability and quality of retrieval, and the information transmitted by the network [1]. The study of attractor neural networks has often been guided by the search for networks of optimal performance.

It has been argued recently that mutual information is the most appropriate concept to measure the performance quality, especially in sparsely coded networks [2,3]. An attempt has been made to infer the Hamiltonian, or energy function, of an optimally performing three-state network from the structure of the initial mutual information and a disordered Blume-Emery-Griffiths (BEG) ([4,5] and references therein) network model has been obtained. This has been used to derive the specific properties that characterize the performance of an extremely diluted network [6]. The arguments leading to the BEG Hamiltonian and the dynamical behavior in networks of other architecture have been studied recently [7,8].

A characteristic feature of the model is to store and retrieve patterns and some of their fluctuations giving rise, in the thermodynamic limit, to two independent local random fields. In contrast to the usual three-state network [9,10], both fields are self-adjusting functions and the network does not need an externally adjustable threshold parameter to activate the neuron states.

One of the further interesting aspects of the model is the presence of an independent order parameter macroscopically characterizing these fluctuations that could yield a new information carrying phase. However, neither the time evolution of this order parameter nor the stability of such a phase have been studied before. The purpose of the present paper is precisely to investigate these points in the extremely diluted network, which has

an exactly solvable dynamics. This also allows one to figure out the size of the basins of attraction, a point that has not been emphasized before, and that can only be studied to some extent in the diluted network due to the complexity of the interactions in the underlying model.

The motivation for our work is the discovery of moderately and, eventually, very long transients in the dynamic evolution of some of the states of the network and the recognition that these states often drive the network into a retrieval phase. It also turned out that these states are not stable in the absence of synaptic noise (temperature  $T$ ), in contrast to an earlier claim [6], but that a finite, activity dependent, threshold value for  $T$  is required for these states to stabilize. We also produce a further comparison of the performance of the network with other three-state networks. Preliminary results of this work have been presented recently [11].

The outline of the paper is the following. In Sec. II we summarize briefly the model and refer the interested reader to previous works for further discussion [6,7]. In Sec. III we state the macrodynamics and we present our results in Sec. IV, ending with our conclusions in Sec. V.

## II. THE MODEL

We consider a three-state network with symmetrically distributed neuron states  $\sigma_{i,t} = 0, \pm 1$  on sites  $i = 1, \dots, N$ , at time step  $t$ , where  $\sigma_{i,t} = \pm 1$  denote the active states. A set of  $p$  ternary patterns,  $\{\xi_i^\mu = 0, \pm 1\}$ ,  $\mu = 1, \dots, p$ , where  $\xi_i^\mu = \pm 1$  are the active ones, are assumed to be independent random variables following the probability distribution

$$p(\xi_i^\mu) = a\delta(|\xi_i^\mu|^2 - 1) + (1 - a)\delta(\xi_i^\mu), \quad (1)$$

where the average  $a = \langle (\xi_i^\mu)^2 \rangle$  is the activity of the patterns. These patterns are embedded in the network by

---

\*Permanent Address: G.Nadjakov Inst. Solid State Physics, Bulgarian Academy of Sciences, 1784 Sofia, Bulgaria

means of a generalized learning rule together with a set  $\{\eta_i^\mu\}$  of normalized fluctuations,  $\eta_i^\mu = ((\xi_i^\mu)^2 - a)/a(1-a)$ , of the binary patterns  $(\xi_i^\mu)^2$  about their average.

The learning rule consists of two Hebbian-like parts

$$J_{ij} = \frac{1}{a^2 N} \sum_{\mu=1}^p \xi_i^\mu \xi_j^\mu, \quad K_{ij} = \frac{1}{N} \sum_{\mu=1}^p \eta_i^\mu \eta_j^\mu, \quad (2)$$

which are the random interactions in the bilinear BEG network with the dynamic variables  $\sigma_{i,t}$  and  $\sigma_{i,t}^2$ , respectively [6]. These are then used to construct the random local fields

$$h_{i,t} = \sum_{j=1}^N J_{ij} \sigma_{j,t}, \quad \theta_{i,t} = \sum_{j=1}^N K_{ij} \sigma_{j,t}^2, \quad (3)$$

where the first one is the usual local field for a three-state network. This enables one to obtain an effective single-site energy function for neuron  $i$ , in mean-field theory,

$$\epsilon_{i,t} = -[h_{i,t} \sigma_{i,t} + \theta_{i,t} \sigma_{i,t}^2] \quad (4)$$

which rules the state-flip probability

$$p(\sigma_{i,t+1} | \{\sigma_{i,t}\}) = \exp(-\beta \epsilon_{i,t}) / Z_t, \quad (5)$$

that specifies the parallel stochastic dynamics for the model, where  $Z_t = 1 + 2e^{\beta \theta_t} \cosh(\beta h_t)$  and  $\beta = a/T$  is the inverse temperature (noise) parameter.

In the sequel we do not indicate the explicit  $t$ -dependence. In distinction to the usual three-state model [9,10], where the coefficient of the quadratic part in  $\epsilon_i$  is an externally adjustable threshold parameter, we have here a self-adjusting, state and pattern dependent function  $\theta_i(\{\sigma_j\}, \{\eta_k^\mu\})$ . In this sense, the present model belongs to a wider class of “self-control” networks, a case of which has been discussed before [2]. We remark, however, that the threshold  $\theta$  used in the latter is a macroscopic parameter, thus, no average had to be done over the microscopic random variables at each time step  $t$ .

Next, we consider the relevant quantities that describe the performance of the network. We need the conditional probability distribution of a neuron state given the distribution of the patterns,  $p(\sigma_i | \xi_i^\mu)$ . As a consequence of the mean-field theory character of the model it is enough to consider the distribution of a single typical neuron, so we can omit the index  $i$ . We can then derive [12]

$$p(\sigma | \xi^\mu) = (s_\xi + m^\mu \xi^\mu \sigma) \delta(\sigma^2 - 1) + (1 - s_\xi) \delta(\sigma), \quad (6)$$

where

$$s_\xi = s^\mu + l^\mu (\xi^\mu)^2, \quad s^\mu = \frac{q - a n^\mu}{1 - a}, \quad l^\mu = \frac{n^\mu - q}{1 - a}. \quad (7)$$

Here,  $m^\mu = \langle \langle \sigma \rangle_{\sigma | \xi} \xi^\mu / a \rangle_\xi$  is the thermodynamic limit  $N \rightarrow \infty$  of the retrieval overlap

$$m_N^\mu = \frac{1}{aN} \sum_i \sigma_i \xi_i^\mu \quad (8)$$

between the state of the network and pattern  $\{\xi_i^\mu\}$ , and the internal average is over the conditional probability. The other parameters are the thermodynamic limits  $q = \langle \langle \sigma^2 \rangle_{\sigma | \xi} \rangle_\xi$  and  $n^\mu = \langle \langle \sigma^2 \rangle_{\sigma | \xi} (\xi^\mu)^2 / a \rangle_\xi$ , of the neural activity

$$q_N = \frac{1}{N} \sum_i \sigma_i^2 \quad (9)$$

and the activity overlap [3,6]

$$n_N^\mu = \frac{1}{aN} \sum_i \sigma_i^2 (\xi_i^\mu)^2, \quad (10)$$

respectively. Finally,  $l^\mu = \langle \langle \sigma^2 \rangle_{\sigma | \xi} \eta^\mu \rangle_\xi$ , is the thermodynamic limit of the *fluctuation overlap* between the binary state variable  $\sigma_i^2$  and  $\eta_i^\mu$  defined as,

$$l_N^\mu = \frac{1}{N} \sum_i \sigma_i^2 \eta_i^\mu. \quad (11)$$

As is clear from its definition, the fluctuation overlap is connected with the activity overlap.

An underlying assumption that leads to the BEG model and that should be preserved in the implementation for any network architecture is that the dynamic activity  $q \sim a$ , as far as the order of magnitude is concerned. The necessity of such an activity control system has been emphasized before (cf. [2,13] and references therein).

The fluctuation overlap  $l^\mu$  can be viewed as the retrieval overlap between the binary patterns  $\{\eta_i^\mu\}$  and states  $\{\sigma_i^2\}$ . A priori, this will be independent of the retrieval overlap  $m^\mu$  between the three-state patterns and states. As will be seen below, a finite non-zero retrieval overlap induces a finite fluctuation overlap, and in this case the parameter  $l^\mu$  should not add anything essentially new to the three-state network. It will turn out, however, that the inverse is in general not true. Indeed,  $l^\mu$  can be finite in a state of dynamic activity without necessarily a finite retrieval overlap  $m^\mu$ . Thus, there can be a phase in which  $m^\mu = 0$  but where, nevertheless, there is a finite information carried by the fluctuation overlap  $l^\mu \neq 0$ . Whether the new phase is actually stable, interesting and how long it takes for the network to reach the corresponding states is the main issue that we address below.

Finally, we consider the mutual information between patterns and neurons, regarding the patterns as the inputs and the neuron states as the output of the network channel at each time step [14,15]. This is given by, recalling that we do not indicate the explicit time dependence,

$$I^\mu(\sigma, \xi^\mu) = S(\sigma) - \langle S(\sigma|\xi^\mu) \rangle_{\xi^\mu}, \quad (12)$$

where

$$S(\sigma) = -q \ln(q/2) - (1-q) \ln(1-q) \quad (13)$$

is the entropy and  $S(\sigma|\xi^\mu)_{\xi^\mu} = aS_a + (1-a)S_{1-a}$  is the equivocation term with

$$S_a = -c_+^\mu \ln c_+^\mu - c_-^\mu \ln c_-^\mu - (1-n^\mu) \ln(1-n^\mu) \\ S_{1-a} = -s^\mu \ln(s^\mu/2) - (1-s^\mu) \ln(1-s^\mu). \quad (14)$$

Here,  $c_\pm^\mu = (n^\mu \pm m^\mu)/2$  and  $s^\mu$  is the parameter in the conditional probability  $p(\sigma|\xi^\mu)$ . The mutual information can then be used to obtain the information  $i^\mu = I^\mu \alpha$ , where  $\alpha = p/N$  is the storage ratio of the network.

### III. MACRODYNAMICS

The local fields in terms of the retrieval and the fluctuation overlaps

$$h_i = \frac{1}{a} \sum_\mu \xi_i^\mu m^\mu, \quad \theta_i = \sum_\mu \eta_i^\mu l^\mu, \quad (15)$$

are the suitable starting point for the macrodynamics [6]. The actual overlaps

$$m^\mu = \langle \overline{\sigma_i} \xi_i^\mu \rangle_\xi, \quad l^\mu = \langle \overline{\sigma_i^2} \eta_i^\mu \rangle_\xi, \quad (16)$$

depend on the thermal averages  $\overline{\sigma_i}$  and  $\overline{\sigma_i^2}$  given by  $F_\beta(h, \theta) = 2e^{\beta\theta} \sinh(\beta h)/Z$  and  $G_\beta(h, \theta) = 2e^{\beta\theta} \cosh(\beta h)/Z$ , respectively. In the zero temperature limit

$$F_\infty = \text{sgn}(h)\Theta(|h| + \theta), \quad G_\infty = \Theta(|h| + \theta). \quad (17)$$

We assume that a single pattern  $\xi^\mu$  and fluctuation  $\eta^\mu$  are condensed, that is,  $m^\mu$  and  $l^\mu$  are of order  $O(1)$  for a given  $\mu = \nu$  (and for  $\mu \neq \nu$  they are of order  $O(1/\sqrt{N})$ ), and we call these  $m$  and  $l$ , respectively. These yield a finite signal term for each local field and related Gaussian noise terms. In accordance with this, we also assume that  $n = n^\nu = O(1)$  and  $s = s^\nu = O(1)$  and we denote  $i = i^\nu$ .

The asymptotic macrodynamics for the extremely diluted network follows then the single-step evolution equations for the order parameters, exact in the large- $N$  limit, for each time step  $t$  [6],

$$m_{t+1} = \int Dy \int Dz F_\beta\left(\frac{m_t}{a} + y\Delta_t; \frac{l_t}{a} + z\frac{\Delta_t}{1-a}\right), \quad (18)$$

$$n_{t+1} = \int Dy \int Dz G_\beta\left(\frac{m_t}{a} + y\Delta_t; \frac{l_t}{a} + z\frac{\Delta_t}{1-a}\right), \quad (19)$$

$$s_{t+1} = \int Dy \int Dz G_\beta\left(y\Delta_t; -\frac{l_t}{1-a} + z\frac{\Delta_t}{1-a}\right), \quad (20)$$

together with the dynamic activity  $q_t = an_t + (1-a)s_t$ . The equation for  $l_t$  is obtained using the relation  $l_t = (n_t - q_t)/(1-a)$ . Here, as usual,  $Dx = \exp(-x^2/2)dx/\sqrt{2\pi}$  whereas  $\Delta_t^2 = \alpha q_t/a^2$  and  $\Delta_t^2/(1-a)^2$  are the variances in the Gaussian local fields  $h_i$  and  $\theta_i$ , respectively. With these equations we also get the time evolution of the information  $i$  by means of Eqs. (12) to (14).

The equations for the dynamics of the macroscopic order parameters can now be used to study both the time evolution of the network and to determine the properties of the stable stationary states.

### IV. RESULTS

We recognize, essentially, three phases given by stable stationary states of the network dynamics Eqs. (18)-(20), as shown in Fig.1, for a typical activity of  $a = 0.8$ . There is a retrieval phase  $R$  ( $m \neq 0, l \neq 0$ ), a fluctuation phase  $Q$  ( $m = 0, l \neq 0$ ) and a self-sustained activity phase  $S$  ( $m = 0, l = 0$ ), referred to as the zero phase,  $Z$ , in previous works [6,11], all for  $q \sim a$ . The stationary states in these phases are indicated as attractors (a) in the side table of the phase diagram. There are also saddle-point solutions (s) either with  $m = 0, l \neq 0, q \sim a$  or with  $m = 0, l = 0, q \sim a$ , denoted also by  $Q$  and  $S$ , respectively. Both the saddle-points in  $Q$  and  $S$  have attractor directions along  $l$ , towards  $l^* \neq 0$  and  $l^* = 0$ , respectively, and repeller directions along  $m$  away from  $m = 0$ . Hence, they have strictly one-dimensional basins of attraction in the two-dimensional order parameter subspace of  $m$  and  $l$ , and then only if the precise initial condition  $m_0 = 0$  is met.

There is a retrieval phase in regions I to V. It is the only stable phase in regions I to III and it coexists with the self-sustained activity phase in regions IV and V. The latter implies that in these two regions the basin of attraction of the retrieval states is always limited by the attracting self-sustained activity states. On the other hand, the fluctuation phase exists only in regions VI and VII, coexisting in the latter with the self-sustained activity phase which, in turn, exists only in that region and in region VIII. Dotted lines in the phase diagram denote continuous phase boundaries while full lines indicate discontinuous transitions. The phase boundaries denoted by thick lines mark the boundary of the retrieval phase, the ones further to the right yield the critical storage capacity  $\alpha_c$ , where both overlaps disappear. Extensive calculations of the  $\alpha$  dependence of the order parameters were performed to obtain the phase diagram, with particular emphasis in the search for possible stable  $Q$  states. Clearly, it can be seen that, for a given activity  $a$ , these states appear only above a certain threshold in  $T$ .

A similar behavior appears for other big values of  $a$  above a minimum, whereas a different behavior sets in for smaller  $a$ , as shown in Fig. 2 for  $T = T(a)$  and  $\alpha = 0$ . Indeed, when  $a$  is less than  $1/2$  there is a continuous phase boundary at  $T = 2/3$  between the retrieval phase at low  $T$  and the self-sustained activity phase at high  $T$ . At  $a = 1/2$  the transition becomes discontinuous and, up to  $a = 0.698$ , the only phases present are still  $R$  and  $S$ . The transition remains discontinuous for small  $\alpha$  and it becomes continuous for bigger values of  $\alpha$ . For  $\alpha = 0$ , the  $Q$  phase starts to appear with increasing  $a$  at a triple point with  $a = 0.698$  and  $T = 0.767$ . Beyond  $a = 0.698$  the transition between the  $R$  and the  $Q$  phase remains discontinuous up to the tricritical point with  $a = 0.711$  and  $T = 0.785$ . For bigger values of  $a$ , the transition between the  $R$  and the  $Q$  phase remains continuous and ends at  $T = 1/2$  for  $a = 1$ . It also turns out that there is a critical  $\alpha = 1/\pi \approx 0.318$ , for  $a = 1$ .

We discuss next the typical  $\alpha$  dependence of the order parameters that yield the phase diagram of Fig. 1 and we also show the information content of the network below and above the threshold where the  $Q$  phase starts to appear. For  $a = 0.8$  where the threshold is given by  $T \approx 0.45$  for  $\alpha = 0.221$ , we obtain the results shown in Fig. 3. Clearly, for  $T$  below that threshold (left figure) the two overlaps  $m$  and  $l$  remain finite together, in a behavior characteristic of retrieval, up to the critical  $\alpha_c$ . Thus, in this regime the fluctuation overlap does not yield anything essentially new that is not contained in the retrieval overlap. In contrast, above the threshold (right figure) the retrieval overlap disappears first with increasing  $\alpha$  leaving a finite  $l \neq 0$  that describes a fluctuation overlap up to a bigger critical value  $\alpha_c$ . Hence, it is necessary that first  $T$  and then  $\alpha$  become large enough for the  $Q$  states to become stable. It is also worth noting that the fluctuation overlap carries a finite information even with zero pattern retrieval overlap. Thus, although the information transmitted by the network is mainly in the retrieval phase, there is also some information due to the  $Q$  phase. This information is provided by the fact that the active neurons coincide with the active patterns but the signs are not correlated. One might imagine an example in pattern recognition where, looking at a black and white picture on a grey background, this phase would tell us the exact location of the picture with respect to the background without finding the details of the picture itself.

We also show in Fig. 3 the comparison of the performance with two other three-state networks. One is the usual network with an externally adjustable optimal threshold parameter [9,10] that appears in the quadratic part of the single-site energy function, formally the same as Eq.(4) but with a uniform  $\theta = \theta_i$ . The parameter is restricted to be positive and chosen to yield the largest mutual information. Allowing the threshold to become negative would essentially mimick a binary model and

this is not the subject of the present work. The second network is a phenomenological extension to finite  $T$  of a recent three-state self-control model (SCT) [3,12] in which the self-control threshold  $\theta_t$  at  $T = 0$  is replaced by a linearly shifted threshold  $\bar{\theta}_t = \theta_t - T$ , where  $\theta_t = \sqrt{2 \ln a} D_t$  with  $D_t^2 = \alpha q_t / a$  being the variance of the noise. The results of Fig. 3 clearly show that the BEG network has a better performance for high  $T$ , at least as far as the information content is concerned, than the optimal threshold network, and a worse performance for lower  $T$ .

To understand the typical behavior of the dynamics of the network we show in Fig.4 the time evolution of the order parameters and the information content, for  $a = 0.8$  and  $T = 0.6$ , in both the BEG and the SCT network. In support of the phase diagram shown in Fig. 1, it can be seen that in the case of the BEG network with increasing  $\alpha$ , one has first the asymptotic states of an  $R$  phase, then the states of a  $Q$  phase and, finally, the states of the  $S$  phase. In all cases where one would expect a  $Q$  state, we start with the most favorable initial overlaps for that state, that is  $m_0 = 0$  and a small but finite  $l$ . In contrast, for the SCT network and the indicated values of  $\alpha$  one has only an  $R$  phase.

A closer examination of the curves for the BEG network reveals that the fluctuation overlap may “drive” a vanishingly small initial retrieval overlap, meaning almost no recognition of a given pattern by the state of the network, into an asymptotic state with finite recognition. This is in contrast with the expectation for other three-state networks, as in the case of the SCT network, where first the overlap  $m_t$  becomes non-zero. It is also worth noting that, with a very small initial  $m_0$ , the states of the network are expected to pass through the vicinity of a saddle point, with a finite fluctuation overlap  $l$  and still a vanishing retrieval overlap at small or intermediate times. This situation is described by the first plateaus in  $q$ ,  $l$  and  $i$ . It is only in passing beyond those plateaus, which may take a rather long time, that the states attain the asymptotic behavior of the retrieval phase. It also turned out that with the initial conditions used for the BEG network, in the left part of the figure, there is no retrieval in the SCT network, meaning that the basins of attraction for retrieval are larger in the BEG network.

Finally, the results for the stationary states are confirmed by a set of flow diagrams, a particular one is shown in Fig. 5 for  $a = 0.8$  and  $T = 0.6$ , first below the  $R$ - $Q$  phase boundary, where the retrieval state  $R$  is stable, and then above, where the  $Q$  phase is stable. Clearly, in the first case, for a small initial retrieval overlap and a finite fluctuation overlap, the states evolve first in the attractor direction of the saddle point and only then they start to flow towards the true (retrieval) attractor. Similar flow diagrams were obtained for other sets of parameters and in all cases we found that the attractors have fairly large basins of attraction.

## V. CONCLUSIONS

We discussed the dynamic evolution and the stationary states of the recently introduced BEG neural network model for an extremely diluted architecture. We made particular emphasis on the stability of the stationary states, which had not been explored before, and found that the new phase  $Q$  (called previously, the “dipolar” or “quadrupolar” phase), characterized by a zero retrieval overlap and a finite fluctuation overlap, is a true stable phase only for moderately to large pattern activity  $a$ . We found that an activity dependent synaptic noise has a relevant role in deciding whether the new phase can be reached or not. In particular, that phase is not a stable one at  $T = 0$  for any activity smaller than one. It is also not stable, in general, for somewhat higher values of  $T$ .

We also found that the dynamics may be slowed down due to the presence of saddle-point solutions in the equations that appear in large regions of the phase diagram, in particular in the retrieval phase and close to the critical phase boundary. Although the specific results obtained here are for the extremely diluted network, some of the features found may also appear in other architectures, for instance, in a layered network, and there is work in progress for that case [8]. It would be interesting to study the time evolution of the BEG network also in other non-trivial dynamics.

## ACKNOWLEDGMENTS

One of the authors (DB) wants to thank T. Verbeiren and J. Busquets Blanco for critical discussions and the Fund for Scientific Research-Flanders, Belgium, for financial support. DRDC acknowledges a Ramón y Cajal grant from the Spanish Ministry of Science (MCyT), and thanks the K.U.Leuven, Belgium, for a visiting grant. EK warmly thanks for hospitality the Abdus Salam International Center, for Theoretical Physics, Trieste, and is financially supported by a grant DGI (MCyT) BFM 2001-291-C02-01. The work of WKT is partially supported by the Conselho Nacional de Desenvolvimento Científico e Tecnológico (CNPq), Brazil, and the same author thanks the Fundação de Amparo à Pesquisa do

Estado de Rio Grande do Sul (FAPERGS), Brazil, for a Visitor Scientist grant to the IF-UFRGS.

- 
- [1] J. Hertz, A. Krogh, and R. Palmer, *Introduction to the Theory of Neural Computation* (Addison-Wesley, Reading, MA 1991).
  - [2] D. R. C. Dominguez and D. Bollé, Phys. Rev. Lett. **80**, 2961 (1998).
  - [3] D. Bollé, D. R. C. Dominguez, and S. Amari, Neural Netw. **13**, 455 (2000).
  - [4] M. Blume, V. J. Emery and R. B. Griffiths, Phys. Rev. A **4**, 1071 (1971); M. Blume, Phys. Rev. **141**, 517 (1966); H. W. Capel, Physica **32**, 966 (1966).
  - [5] J. M. de Araújo, F. A. da Costa and F. D. Nobre, Eur. Phys. J. B **14**, 661 (2000).
  - [6] D. R. Carreta Dominguez and E. Korutcheva, Phys. Rev. E **62**, 2620 (2000).
  - [7] D. Bollé and T. Verbeiren, Phys. Lett. A **297**, 156 (2002).
  - [8] D. Bollé, R. Erichsen, Jr., and W. K. Theumann (unpublished).
  - [9] J. S. Yedidia, J. Phys. A **22**, 2265 (1989).
  - [10] D. Bollé, G. M. Shim, B. Vinck, and V. A. Zagrebnov, J. Stat. Phys. **74**, 565 (1994).
  - [11] D. R. C. Dominguez, E. Korutcheva, W. K. Theumann, and R. Erichsen Jr., Proceedings of the International Conference on Artificial Neural Networks, ICANN-2002 (Lecture Notes in Computer Science, Springer-Verlag, to be published).
  - [12] D. Bollé and D. Dominguez Carreta, Physica A **286**, 401 (2000).
  - [13] M. Okada, Neural Netw. **9**, 1429 (1996).
  - [14] C. E. Shannon, Bell Syst. Techn. J. **27**, 379 (1948).
  - [15] R. E. Blahut, *Principles and Practice of Information Theory* (Addison-Wesley, Reading, MA 1990), Chapter 5.

	I	II	III	IV	V	VI	VII	VIII
R	a	a	a	a	a	-	-	-
Q	s	s	-	-	s	a	a	-
S	-	s	s	a	a	-	a	a

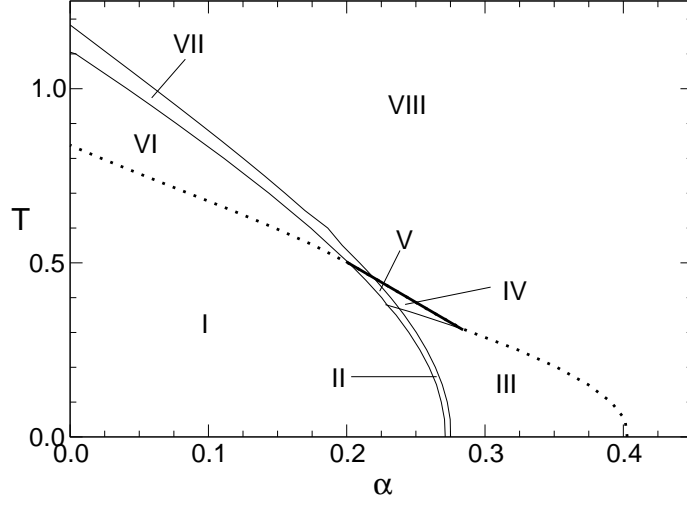


FIG. 1. The  $(T, \alpha)$  phase diagram for the extremely diluted BEG network with pattern activity  $a = 0.8$ . Full (dotted) lines denote discontinuous (continuous) transitions. The heavy lines denote the boundary of the retrieval phase R and the other lines the boundaries of the fluctuation-overlap phase Q and the self-sustained activity phase S. The solutions are either attractors (a) or saddle points (s) .

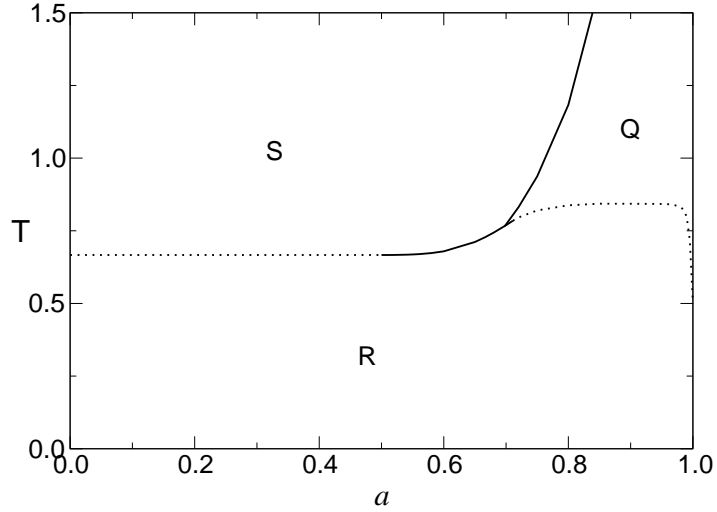


FIG. 2. The  $(T, a)$  phase diagram for the extremely diluted BEG network with the load  $\alpha = 0$ . Full (dotted) lines denote discontinuous (continuous) transitions .

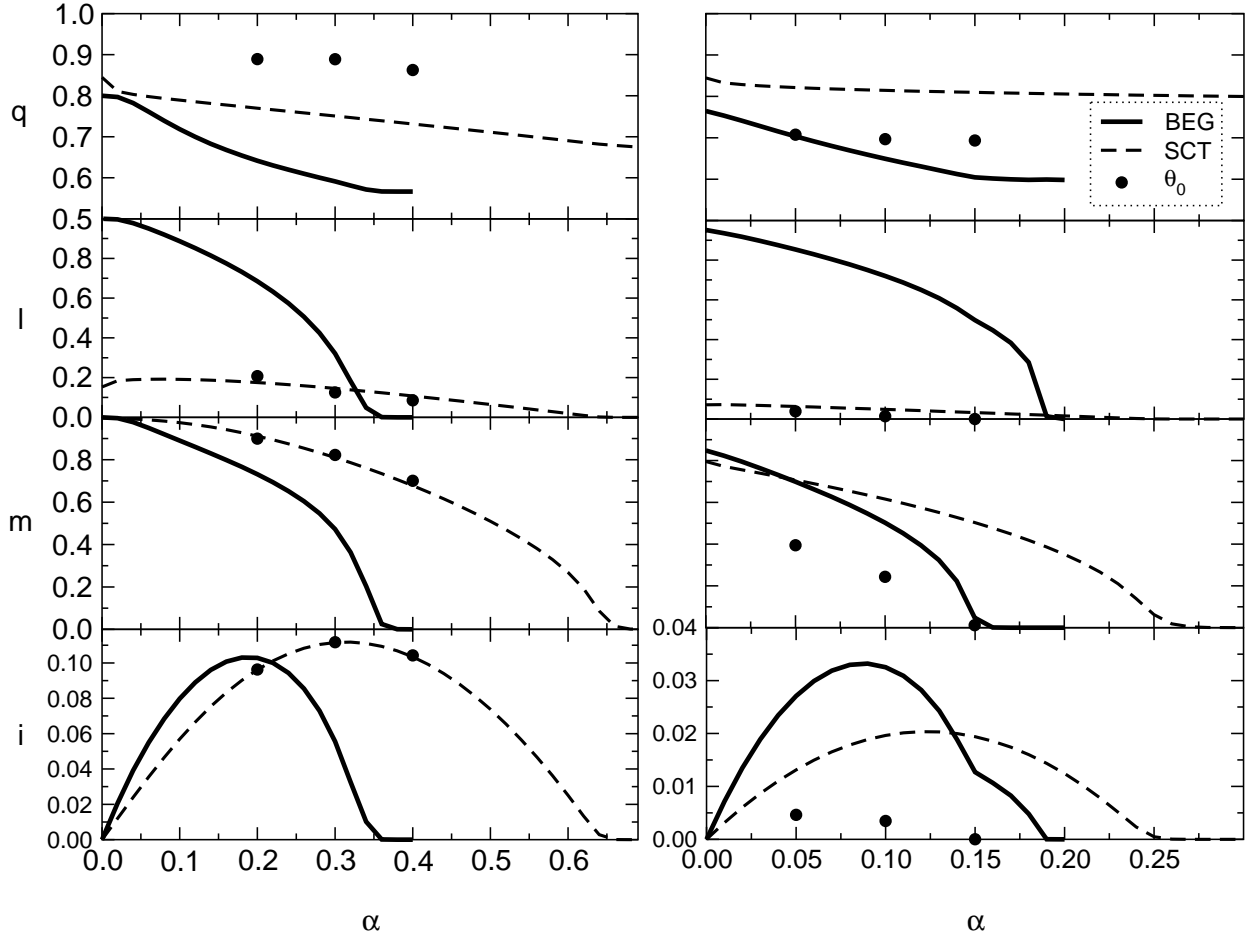


FIG. 3. The order parameters  $m$ ,  $l$ , and  $q$ , and the information content  $i$ , in the stationary state, for initial overlaps  $m_0 = 1$ ,  $l_0 = 1$  and  $q_0 = a$ , as functions of the load  $\alpha$ , for the BEG network with pattern activity  $a = 0.8$  and two noise levels:  $T = 0.2$  (left) and  $T = 0.6$  (right). The self-controlled threshold network (SCT), in dashed lines, and the optimal threshold network (dots), are also shown.

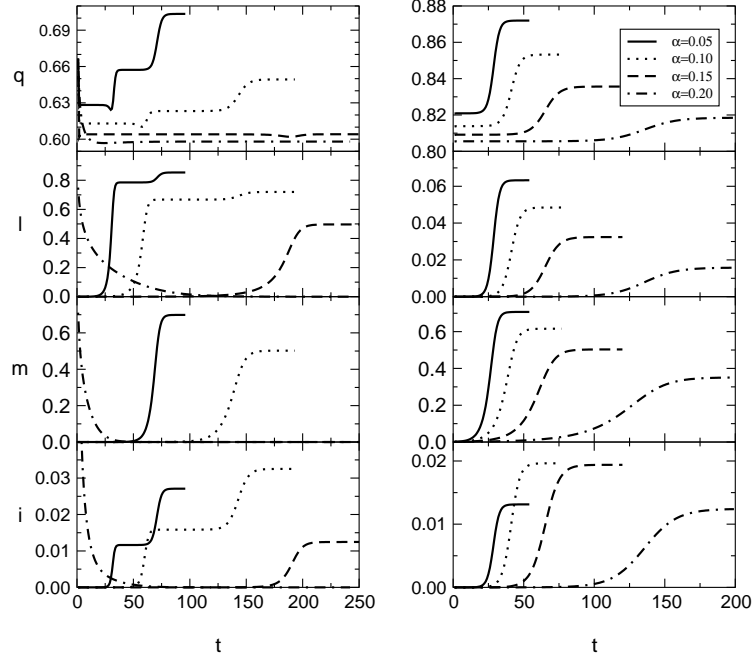


FIG. 4. Time evolution of the order parameters  $m$ ,  $l$  and  $q$  and information content  $i$ , for pattern activity  $a = 0.8$ , temperature  $T = 0.6$  and load  $\alpha$ , as indicated. The BEG network (left), for the initial overlaps  $m_0 = l_0 = 10^{-5}$ , except for  $\alpha = 0.2$  ( $m_0 = l_0 = 1$ ); the SCT network (right), for the initial overlaps  $m_0 = 10^{-3}$  and  $l_0 = 1$ ; both with  $q_0 = a$ .

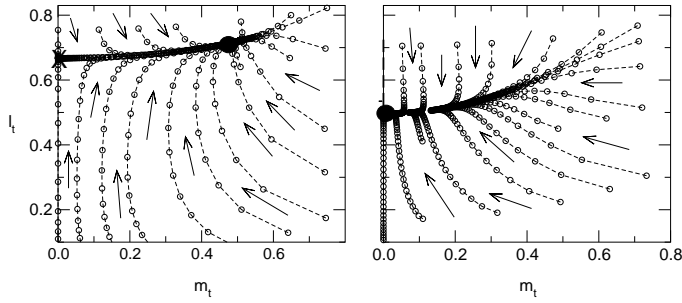


FIG. 5. The flow diagram  $(l, m)$  for the BEG network with  $a = 0.8$  and  $T = 0.6$ . For  $\alpha = 0.1$  (left) the stable attractor is  $R$ , indicated by the circle, while  $Q$ , indicated by the cross, is a saddle point. For  $\alpha = 0.15$  (right) the stable attractor is  $Q$ .